APPLIED AND ENVIRONMENTAL MICROBIOLOGY, June 1995, p. 2252–2256 Vol. 61, No. 6
0099-2240/95/$04.00+0

Nonuniform Spatial Patterns of Respiratory Activity within Biofilms during Disinfection

CHING-TSAN HUANG,[1] F. PHILIP YU,[1,2]† GORDON A. MCFETERS,[1,2] AND PHILIP S. STEWART[1,3]*

Center for Biofilm Engineering,[1] Department of Microbiology,[2] and Department of Chemical Engineering,[3] Montana State University, Bozeman, Montana 59717

Received 21 November 1994/Accepted 13 March 1995

Fluorescent stains in conjunction with cryoembedding and image analysis were applied to demonstrate spatial gradients in respiratory activity within bacterial biofilms during disinfection with monochloramine. Biofilms of *Klebsiella pneumoniae* and *Pseudomonas aeruginosa* grown together on stainless steel surfaces in continuous-flow annular reactors were treated with 2 mg of monochloramine per liter (influent concentration) for 2 h. Relatively little biofilm removal occurred as evidenced by total cell direct counts. Plate counts (of both species summed) indicated an average 1.3-log decrease after exposure to 2 mg of monochloramine per liter. The fluorogenic redox indicator 5-cyano-2,3-ditolyl tetrazolium chloride (CTC) and the DNA stain 4′,6-diamidino-2-phenylindole (DAPI) were used to differentiate respiring and nonrespiring cells in biofilms. Epifluorescence micrographs of frozen biofilm cross sections clearly revealed gradients of respiratory activity within biofilms in response to monochloramine treatment. These gradients in specific respiratory activity were quantified by calculating the ratio of CTC and DAPI intensities measured by image analysis. Cells near the biofilm-bulk fluid interface lost respiratory activity first. After 2 h of biocide treatment, greater respiratory activity persisted deep in the biofilm than near the biofilm-bulk fluid interface.

Microbial biofilms are implicated in many industrial fouling, corrosion, and hygiene problems. The main strategy of biofilm control is the use of chemical biocides to kill the attached microorganisms and/or remove them from the surface. Unfortunately, bacteria in biofilms are usually found to be many times more difficult to eradicate than their planktonic counterparts (1, 5, 7, 9, 17, 20). The relative resistance of biofilm microorganisms has tremendous economic and environmental ramifications in applications as diverse as cooling water, papermaking, medical implants, drinking-water distribution, secondary oil recovery, metalworking, and food processing (2, 10).

In studies to determine the underlying basis for biofilm recalcitrance, researchers at the Center for Biofilm Engineering and elsewhere have concluded that spatial information about biocide and physiological gradients inside biofilms is necessary to address this problem (13, 24). For example, a direct measurement of profound gradients in chlorine concentration within biofilms in flowing systems with a chlorine microelectrode has recently been reported (8). Equally valuable would be the spatial patterns of physiological activity within biofilms in response to biocide treatment.

There are few reports of spatial gradients of physiological activity within biofilms obtained by direct-measurement approaches. Kinniment and Wimpenny measured a gradient in adenylate charge within a biofilm by determining the energy charges in frozen sections taken at different depths of the interfacial community (12). Zhang and Bishop used microslicing and phospholipid analysis to investigate the spatial distribution of biofilm properties (34). The use of scanning confocal laser microscopy in conjugation with fluorescent probes is one of the most attractive approaches to reveal spatial gradients within biofilms (3, 4, 13, 15). For example, Korber et al. recently described gradients in nucleic acid staining and cell length in a biofilm treated with fleroxacin (13). This technique involves relatively expensive instrumentation and may be unsuitable for the study of thick or opaque biofilms. Researchers working with artificially immobilized cells have also developed techniques for the visualization of gradients in nucleic acid concentrations as well as in protein and DNA synthesis rates (11, 14, 18, 19, 25, 26). Many of these approaches, however, are unable to reflect the action of biocides or are not readily applicable to natural biofilms.

The purpose of the work reported in this article was to test the hypothesis that disinfection of a biofilm results in a nonuniform spatial loss of physiological activity. We describe the coupling of the fluorescent redox dye 5-cyano-2,3-ditolyl tetrazolium chloride (CTC) with cryosectioning and image analysis to demonstrate the nonuniform loss of respiratory activity in biofilms treated with monochloramine.

MATERIALS AND METHODS

Bacterial strains and growth conditions. *Klebsiella pneumoniae* (Kp1), isolated from drinking water, was obtained from D. Smith, South Central Connecticut Water Authority, New Haven, Conn. An environmental isolate of *Pseudomonas aeruginosa* (ERC1) was taken from the culture collection at the Center for Biofilm Engineering. A phosphate-buffered (pH 7.2) minimal salts medium (6, 29) with 20 mg of glucose per liter as the sole carbon source was used to grow biofilms. Reactor effluent was homogenized with a tissue homogenizer to disperse cell aggregates and then plated on R2A (Difco) agar to monitor the growth of biofilm bacteria and to check for contamination on a daily basis. Both *K. pneumoniae* and *P. aeruginosa* were identified and differentiated by colony shading and morphology. The colonies of Kp1 appeared opaque white with a smooth, round edge, while ERC1 formed a translucent, creamy white colony with an irregular shape. Steady state was reached after 7 to 10 days of operation, as reflected by a constant concentration of cells in the reactor effluent.

Biofilm apparatus. Biofilms were grown on 316L stainless steel slides in an annular reactor (23). The average area of the stainless steel slide covered with biomass was 31.5 cm^2. The operating conditions of the reactor system have been described in detail previously (6). The annular reactor contained 12 removable slides which were positioned around the inside wall of the outer drum. The inner cylinder of the annular reactor rotated at 150 rpm to produce a uniform shear stress over the area on which biofilms were grown. The fluid volume in the reactor was 600 ml. The reactors were operated at a dilution rate of 3.2 h^{-1}. This

* Corresponding author. Phone: (406) 994-2890. Fax: (406) 994-6098. Electronic mail address: phil_s@erc.montana.edu.

† Present address: Nalco Chemical Company, Naperville, IL 60563.

dilution rate greatly exceeds the growth rate of planktonic cells in the reactor ($<0.15\ h^{-1}$) and thus ensures that the activity of biofilm microorganisms dominates that of suspended cells in the system.

Disinfection of biofilms. The disinfectant used was monochloramine at a concentration of 2 mg of chlorine per liter (influent concentration); the monochloramine was made with sodium hypochlorite and ammonium chloride (16). A pulse of concentrated disinfectant sufficient to raise the bulk concentration to 2 mg/liter was added to the bulk fluid in the reactor. The pulse was simultaneously accompanied by the steady addition of biocide in the influent at 2 mg/liter. The combined effect of this dosing protocol is to induce an abrupt step change in the disinfectant concentration in the system. The biofilm slides were exposed to monochloramine in the reactor at 25°C. The monochloramine concentration was measured with an *N,N*-diethyl-*p*-phenylenediamine (DPD) chlorine test kit (Hach Co., Loveland, Colo.).

Respiratory activity assessment. Biofilms were collected by withdrawing slides after 0, 30, 60, 90, and 120 min of disinfection. The slides were then placed in a staining container with the biofilm side up, and the disinfectant was neutralized by immersion in sodium thiosulfate (0.01% final concentration). Respiratory activity within biofilms was determined with CTC (Polysciences, Inc.) by a procedure reported by Rodriguez et al. (21, 22) with minor modifications (32). The biofilm slides were immersed in 0.05% CTC solution for 2 h at 25°C. The specimens were fixed with formalin (5% final concentration) and then immediately stained with 1 μg of 4′,6-diamidino-2-phenylindole (DAPI) (Sigma Chemical Co.) per ml (final concentration) for 5 min. The biofilms were embedded and removed from the substratum by a cryoembedding technique (31) with Tissue-Tek OCT compound (Miles Inc.). The specimen was then wrapped in aluminum foil and stored at −70°C before cryotomy. Frozen sections were cut with a cryostat (Reichert-Jung Cryocut 1800; Leica) operated at −19°C. The sections (5 μm thick) were collected with glass slides for examination by epifluorescence microscopy.

The sections were examined with an Olympus BH-2 microscope with epifluorescence illumination (100-W mercury lamp). An Olympus B filter cubic unit with an excitation filter (BP490), a dichroic mirror (DM500), and a barrier filter (AFC+O515) was used to simultaneously visualize the CTC-formazan and DAPI fluorescence within the sectioned biofilms by the distinctive color of each stain. The nonrespiring bacteria appeared green when stained with DAPI, whereas the respiring cells were green but contained intracellular crystals of red CTC-formazan. Filter block G fitted with an O590 barrier filter was used to visualize the red CTC-formazan crystals by excluding DAPI fluorescence, whereas a U excitation filter cubic unit with an excitation filter (UG-1), a dichroic mirror (DM 400), and a barrier filter (L420) was used for visualizing the DAPI fluorescence alone.

Enumeration. Biofilm bacteria in monochloramine-treated and untreated samples were assayed by scraping the biofilms off the slide followed by disaggregation of the cell suspension in an ice bath for 3 min with a homogenizer (Tekmar), enumeration by serial dilution, and plating on R2A agar. The phrase "total culturable-cell count" is used to indicate that CFUs for both species were summed. The areal density of biofilm bacteria on the substratum is expressed as CFU per square centimeter. Total cell numbers were obtained by enumerating DAPI-stained samples collected on black polycarbonate membranes (0.2 μm; Nuclepore).

Image analysis. An American Innovision image-processing system that consisted of a Pulnix color charge-coupled device camera (1.5 lx) with a resolution of 512 by 400 pixels for image capture was used. The software was run on an IBM-clone personal computer, which converted the epifluorescence micrograph into a digitized image. Conversion of pixel unit to length (in micrometers) was accomplished by calibration with a stage micrometer. The digitized-image area was 45,740 μm^2.

The stored images from the American Innovision system were converted to a tagged image file format (TIFF) and then analyzed with MARK software on a Hewlett Packard 9000/730 workstation. The MARK program was developed by Gary Harkin of the Center for Biofilm Engineering at Montana State University. Selected areas of the DAPI and CTC-formazan images could then be analyzed to calculate the total intensity or could be superimposed to determine the ratio of intensities of the two fluorochromes.

Statistical analysis. The experiment was repeated three times. The microscopic enumeration results were obtained in each experiment from counts of 10 microscopic fields, and plate count data for three plates were averaged. At each time point in each experiment, the mean counts for total cells, culturable Kp1 cells, culturable ERC1 cells, and total culturable cells (Kp1 plus ERC1) were recorded. Statistical analyses were performed with S-Plus software (version 3.1 by Statistic Science, Inc., Seattle, Wash.) and were based upon the log transformational means.

RESULTS

Cell counts. The decreases in total cell direct counts and the plate counts of attached cells during exposure to 2 mg of monochloramine per liter are shown in Fig. 1. The initial total cell density on the slide before treatment was 9.13 ± 0.15 log cells per cm^2 (± the standard error), while the mean concentrations of culturable cells were 8.94 ± 0.23 log CFU/cm^2 for *K. pneumoniae* Kp1 and 8.22 ± 0.05 log CFU/cm^2 for *P. aeruginosa* ERC1. Differences in the enumeration of unexposed cell populations at time zero between total cells and total culturable cells were not statistically significant (two-sample test; $P > 0.7$). After a 2-h treatment, only a 0.3-log decrease in total cell direct count was observed, whereas a 1.3-log reduction for Kp1, a 1.1-log reduction for ERC1, and a 1.3-log reduction for total culturable cells were detected by plate counts. The difference between total cells and total culturable cells after a 2-h disinfection was statistically significant (two-sample test; $P < 0.01$).

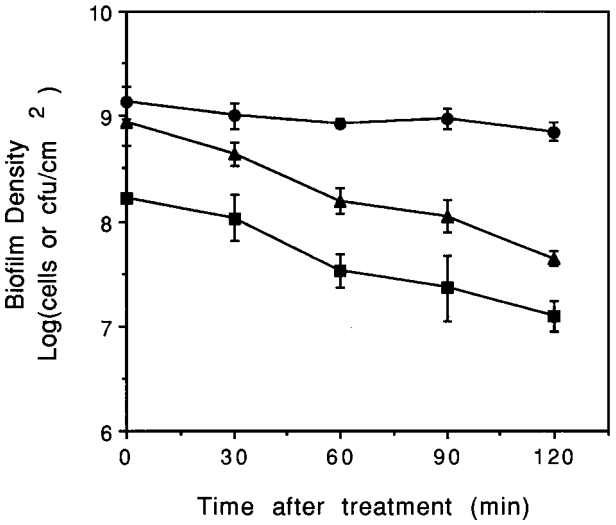

FIG. 1. Cell count results of biofilms treated with 2 mg of monochloramine per liter. ●, total cell direct count; ▲, *K. pneumoniae* Kp1; ■, *P. aeruginosa* ERC1. ($n = 3$; bars indicate standard errors.)

Epifluorescent micrographs. CTC and DAPI were employed to determine the effect of monochloramine on bacterial respiratory activity within biofilms. Respiring cells within biofilms reduced CTC to red CTC-formazan intracellular crystals, while both respiring and nonrespiring cells stained green with DAPI. By cryosectioning techniques, the spatial distribution of respiring and nonrespiring cells within biofilms could be observed by epifluorescent microscopy. Figure 2 illustrates representative patterns of respiratory activity within biofilms in response to treatment with 2 mg of monochloramine per liter. Respiring cells dominated most of the biofilm before disinfection (Fig. 2a). Bacteria within the untreated biofilm appeared uniformly red at this stage because the CTC staining was more intense than the DAPI staining. As disinfection proceeded, respiratory activity diminished and the combination of stains yielded a yellow color. Figure 2b shows that nonrespiring (green) cells started to appear at the biofilm-bulk liquid interface after 30 min of treatment. After a 1-h disinfection, nonrespiring cells constituted a significant fraction of the biofilm and some of the biofilm biomass was detached (Fig. 2c). At the end of the experiment, only a small fraction of the biofilm retained respiratory activity (Fig. 2d) and parts of the biofilm were entirely green (micrograph not shown), indicating a complete absence of respiratory activity. The loss of respiratory activity in the biofilm was not spatially uniform. Most of the respiratory activity loss occurred near the biofilm-bulk fluid interface.

Image analysis. Image analysis was used to illustrate the response of bacteria in biofilms with exposure to monochlora-

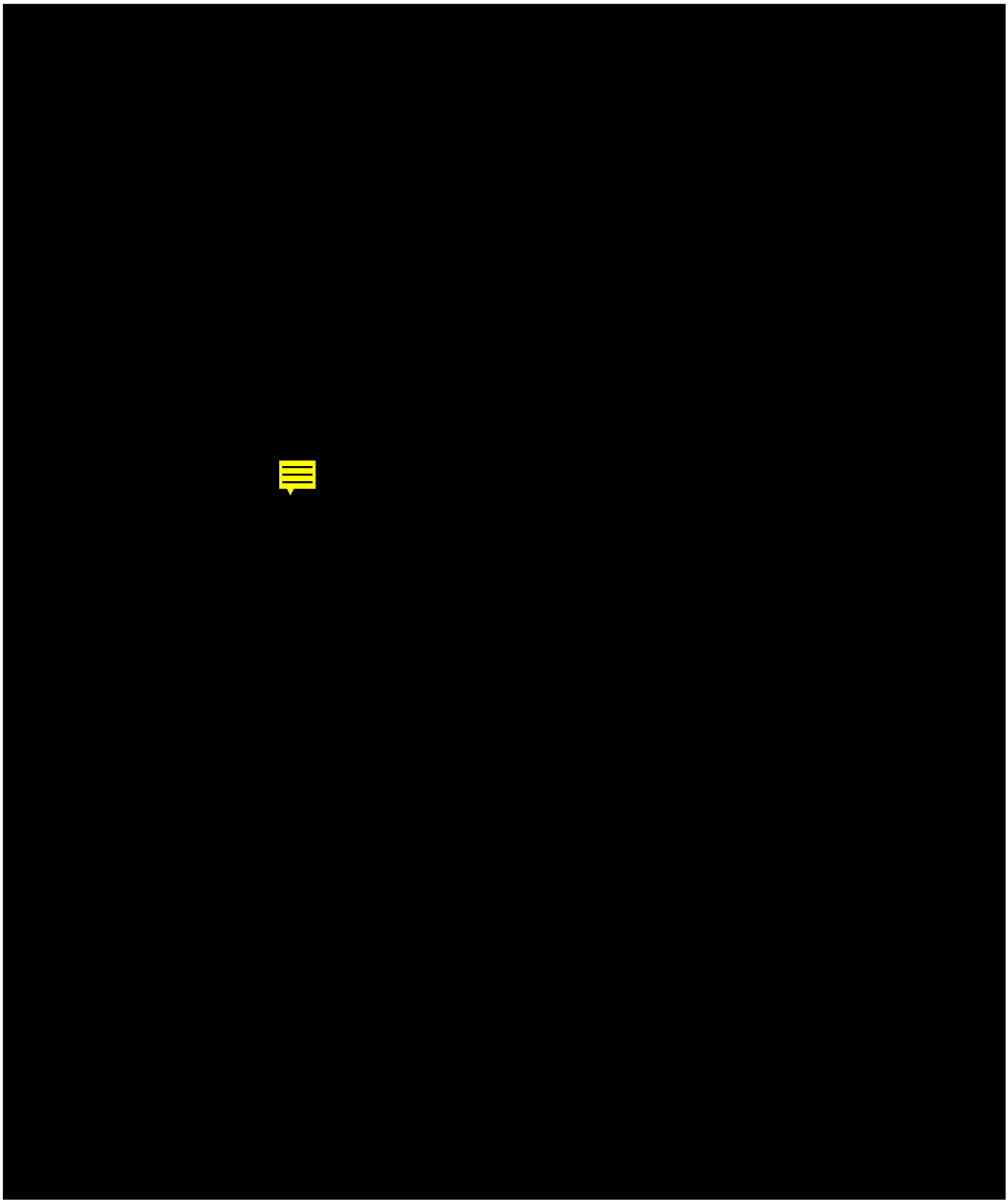

FIG. 2. Epifluorescence micrographs of frozen sections of a mixed *K. pneumoniae* Kp1 and *P. aeruginosa* ERC1 biofilm grown on stainless steel treated with 2 mg of monochloramine per liter. (a) Before treatment; (b) after a 30-min treatment; (c) after a 60-min treatment; (d) after a 120-min treatment. The orientation of the biofilm was such that the substratum was at the bottom and the biofilm-bulk liquid interface was at the top in each micrograph. Bar = 25 μm.

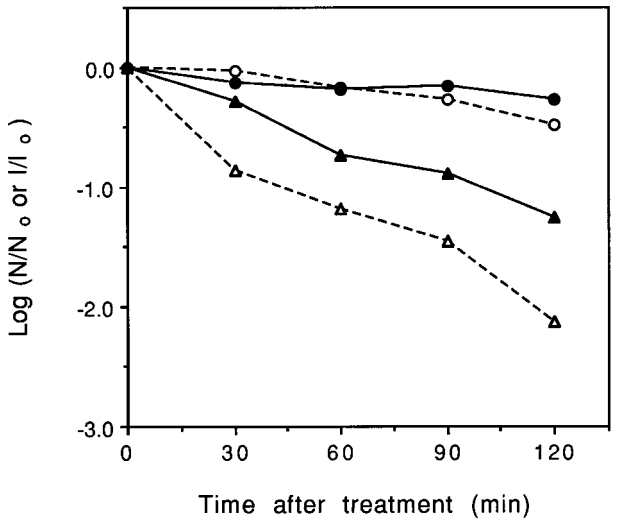

FIG. 3. Responses of biofilms treated with 2 mg of monochloramine per liter to different methods of determining bacterial density and activity. ●, total cell direct count; ▲, total culturable-cell count; ○, DAPI; △, CTC-formazan. N/N_0 and I/I_0, respectively, are the count and intensity measurements normalized by the initial count or intensity.

mine (Fig. 3). The numerical values in biofilm staining intensity images for intracellular CTC-formazan (respiratory activity) and DAPI (total cells) were averaged for 10 different frames. Values for CFUs and total microscopic direct counts are also shown in Fig. 3. The change in total or community DAPI intensity agreed well with total cell direct-count results. A 2.1-log decrease in CTC-formazan intensity after 2 h of treatment was observed, while only a 1.2-log decrease in the number of culturable cells (Kp1 and ERC1) was detected.

The ratio of CTC-formazan to DAPI intensity was used as an indicator of specific respiratory activity locally within the biofilm. Figure 4 illustrates a gradient of specific respiratory activity measured at intervals during monochloramine treatment. The biofilm thicknesses, as determined by the dimension of the DAPI-stained region, were 121, 116, 106, 125, and 92 μm at treatment times of 0, 30, 60, 90, and 120 min, respectively. The curves in Fig. 4 are not derived from the same spot of biofilm since the technique is destructive. Rather, the data in Fig. 4 show representative results. Before the application of monochloramine, CTC-formazan intensity was detected throughout the entire biofilm (a ca. 120-μm range). As chloramination proceeded, the peaks of the CTC-formazan/DAPI ratio shifted toward the substratum and the areas under the peaks decreased. After 120 min of disinfection, only about a 60-μm-thick region of the biofilm exhibited a relatively low level of respiratory activity. The distribution of CTC-formazan and DAPI was similar to that revealed in photomicrographs (Fig. 2).

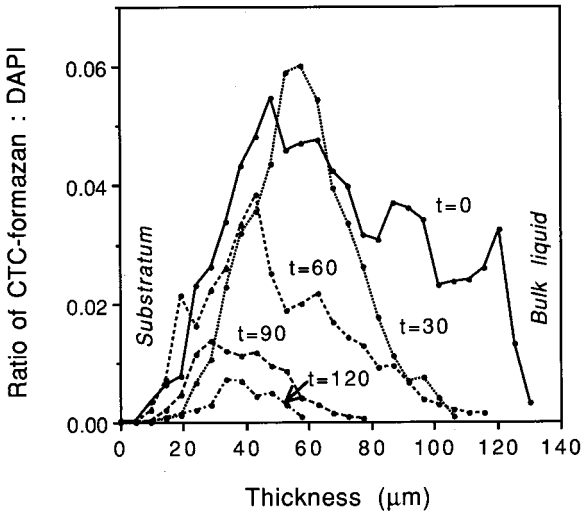

FIG. 4. Ratio of intensities of CTC-formazan and DAPI obtained from 5-μm frozen sections following exposure to 2 mg of monochloramine per liter. The biofilm thicknesses determined by the dimension of the DAPI-stained region were 121 μm before treatment and 116, 106, 125, and 92 μm at 30, 60, 90, and 120 min, respectively. t, time (min).

DISCUSSION

Some new methods to measure biocide efficacy such as bioluminescence with the *lux* gene (30), direct viable count (33), and physiological probes (22, 32) are emerging. These approaches complement the conventional plate count method but suffer one of the same limitations: they average the response over the entire biofilm and thus provide no spatial resolution. When spatial information is important, as it almost certainly is in the question of biofilm resistance to antimicrobial agents, more sophisticated techniques are required. By coupling a biofilm cryosectioning technique (31) with a fluorogenic probe that is specific for bacterial respiratory activity (32), we were able to visualize spatial patterns of respiratory activity within a heterogeneous biofilm community during disinfection.

Spatially nonuniform loss of microbial respiratory activity within the biofilm after treatment with monochloramine was observed. The greatest loss of respiratory activity occurred near the biofilm-bulk fluid interface. Residual respiratory activity was highest near the substratum or in the centers of cell clusters. The spatial distribution of respiratory activity within untreated biofilms was, in contrast, relatively uniform.

There are two mechanisms that could explain such activity gradients after disinfection. The first possible explanation is the depletion of monochloramine in the biofilm interior through a reaction-diffusion interaction. Chen et al. (6) reported evidence of monochloramine concentration gradients in pure-culture *P. aeruginosa* biofilms. Recently, de Beer et al. (8) confirmed the presence of chlorine concentration gradients in biofilms during disinfection with a chlorine microelectrode. Tashiro et al. presented experimental evidence in support of a reaction-diffusion limitation of isothiazolone efficacy (28), and Suci et al. recently demonstrated retarded penetration of a fluoroquinolone antibiotic into biofilms (27). Together, these reports show that incomplete penetration of a biofilm by a reactive biocide is a tenable explanation for the reduced efficacy of such agents against biofilms.

A second mechanism to explain nonuniform biofilm disinfection also stems from a transport limitation. In this case, the reaction-diffusion interaction applies to a growth-limiting nutrient or product, with the result that microorganisms deep in the biofilm grow slowly or not at all. If the slowly growing or starved microorganisms are more resistant to antimicrobial action, physiological gradients would appear during disinfection and would mirror the preexisting growth rate gradient.

The gradients of respiratory activity observed when biofilms were exposed to monochloramine are qualitatively consistent with a transport limitation like either of those described above. In both cases, greater residual activity is expected near the substratum or in microcolony interiors than near the biofilm-

bulk fluid interface, just as observed in our experiments. This result should motivate continued investigation of transport-based explanations for biofilm resistance to biocides.

ACKNOWLEDGMENTS

This work was supported by the Center for Biofilm Engineering at Montana State University, a National Science Foundation-sponsored engineering research center (cooperative agreement EEC-8907039), and by the Center's industrial associates.

We thank Martin Hamilton for advice on statistical analyses and Gayle Callis for expert technical assistance.

REFERENCES

1. **Brown, M. R. W., and P. Gilbert.** 1993. Sensitivity of biofilms to antimicrobial agents. J. Appl. Bacteriol. Symp. Suppl. **74:**87S–97S.
2. **Bryers, J. D.** 1993. Bacterial biofilms. Curr. Opin. Biotechnol. **4:**197–204.
3. **Caldwell, D. E., D. R. Korber, and J. R. Lawrence.** 1992. Imaging of bacterial cells by fluorescent exclusion using scanning confocal laser microscopy. J. Microbiol. Methods **15:**249–261.
4. **Caldwell, D. E., D. R. Korber, and J. R. Lawrence.** 1992. Confocal laser microscopy and digital image analysis in microbial ecology. Adv. Microb. Ecol. **12:**1–67.
5. **Camper, A. K., M. W. LeChevallier, S. C. Broadaway, and G. A. McFeters.** 1986. Bacteria associated with granular activated carbon particles in drinking water. Appl. Environ. Microbiol. **52:**434–438.
6. **Chen, C.-I., T. Griebe, and W. G. Characklis.** 1993. Biocide action of monochloramine on biofilm systems of *Pseudomonas aeruginosa*. Biofouling **7:**1–17.
7. **Costerton, J. W., K.-J. Chen, G. G. Geesey, T. I. Ladd, J. C. Nickel, M. Dasgupta, and T. J. Marrie.** 1987. Bacterial biofilms in nature and disease. Annu. Rev. Microbiol. **41:**435–464.
8. **de Beer, D., R. Srinivasan, and P. S. Stewart.** 1994. Direct measurement of chlorine penetration into biofilms during disinfection. Appl. Environ. Microbiol. **60:**4339–4344.
9. **Herson, D. S., B. McGonigle, M. A. Payer, and K. H. Baker.** 1987. Attachment as a factor in the protection of *Enterobacter cloacae* from chlorination. Appl. Environ. Microbiol. **53:**1178–1180.
10. **Hoyle, B. D., and J. W. Costerton.** 1991. Bacterial resistance to antibiotics: the role of biofilms. Prog. Drug Res. **37:**91–105.
11. **Karel, S. F., and C. R. Robertson.** 1989. Cell mass synthesis and degradation by immobilized *Escherichia coli*. Biotechnol. Bioeng. **34:**337–356.
12. **Kinniment, S. L., and J. W. T. Wimpenny.** 1992. Measurements of the distribution of adenylate concentrations and adenylate energy charge across *Pseudomonas aeruginosa* biofilms. Appl. Environ. Microbiol. **58:**1629–1635.
13. **Korber, D. R., G. A. James, and J. W. Costerton.** 1994. Evaluation of fleroxacin activity against established *Pseudomonas fluorescens* biofilms. Appl. Environ. Microbiol. **60:**1663–1669.
14. **Kuhn, R. H., S. W. Peretti, and D. F. Ollis.** 1991. Microfluorimetric analysis of spatial and temporal patterns of immobilized cell growth. Biotechnol. Bioeng. **38:**340–352.
15. **Lawrence, J. R., D. R. Korber, B. D. Hoyle, J. W. Costerton, and D. E. Caldwell.** 1991. Optical sectioning of microbial biofilms. J. Bacteriol. **173:**6558–6567.
16. **LeChevallier, M. W., C. D. Cawthon, and R. G. Lee.** 1988. Inactivation of biofilm bacteria. Appl. Environ. Microbiol. **54:**2492–2499.
17. **LeChevallier, M. W., T. M. Evans, and R. J. Seidler.** 1981. Effect of turbidity on chlorination efficiency and bacterial persistence in drinking water. Appl. Environ. Microbiol. **42:**159–167.
18. **Monbouquette, H. G., and D. F. Ollis.** 1988. Scanning microfluorimetry of Ca-alginate immobilized *Zymomonas mobilis*. Bio/Technology **6:**1076–1079.
19. **Monbouquette, H. G., G. D. Sayles, and D. F. Ollis.** 1990. Immobilized cell biocatalyst activation and pseudo-steady-state behavior: model and experiment. Biotechnol. Bioeng. **35:**609–629.
20. **Ridgway, H. F., and B. H. Olson.** 1982. Chlorine resistance patterns of bacteria from two drinking water distribution systems. Appl. Environ. Microbiol. **44:**972–987.
21. **Rodriguez, G. G., D. Phipps, K. Ishiguro, and H. F. Ridgway.** 1992. Use of a fluorescent redox probe for direct visualization of actively respiring bacteria. Appl. Environ. Microbiol. **58:**1801–1808.
22. **Schaule, G., H.-C. Flemming, and H. F. Ridgway.** 1993. Use of 5-cyano-2,3-ditolyl tetrazolium chloride for quantifying planktonic and sessile respiring bacteria in drinking water. Appl. Environ. Microbiol. **59:**3850–3857.
23. **Siebel, M. A., and W. G. Characklis.** 1991. Observations of binary population biofilms. Biotechnol. Bioeng. **37:**778–789.
24. **Stewart, P. S.** 1994. Biofilm accumulation model that predicts antibiotic resistance of *Pseudomonas aeruginosa* biofilms. Antimicrob. Agents Chemother. **38:**1052–1058.
25. **Stewart, P. S., S. F. Karel, and C. R. Robertson.** 1991. Characterization of immobilized cell growth rates using autoradiography. Biotechnol. Bioeng. **37:**824–833.
26. **Stewart, P. S., and C. R. Robertson.** 1988. Product inhibition of immobilized *Escherichia coli* arising from mass transfer limitation. Appl. Environ. Microbiol. **54:**2464–2471.
27. **Suci, P. A., M. W. Mittelman, F. P. Yu, and G. G. Geesey.** 1994. Investigation of ciprofloxacin penetration into *Pseudomonas aeruginosa* biofilms. Antimicrob. Agents Chemother. **38:**2125–2133.
28. **Tashiro, H., T. Numakura, T. S. Nishikawa, and Y. Miyaji.** 1991. Penetration of biocides into biofilm. Water Sci. Technol. **23:**1395–1403.
29. **van der Wende, E.** 1991. Biocide action of chlorine on *Pseudomonas aeruginosa* biofilm. Ph.D. dissertation. Montana State University, Bozeman.
30. **Walker, A. J., S. A. A. Jassim, J. T. Holah, S. P. Denyer, and G. S. A. B. Stewart.** 1992. Bioluminescent *Lysteria monocytogenes* provide a rapid assay for measuring biocide efficacy. FEMS Microbiol. Lett. **91:**251–256.
31. **Yu, F. P., G. Callis, P. S. Stewart, T. Griebe, and G. A. McFeters.** 1994. Cryosectioning of biofilms for microscopic examination. Biofouling **8:**85–91.
32. **Yu, F. P., and G. A. McFeters.** 1994. Rapid *in situ* assessment of physiological activities in bacterial biofilms using fluorescent probes. J. Microbiol. Methods **20:**1–10.
33. **Yu, F. P., P. H. Pyle, and G. A. McFeters.** 1993. A direct viable count method for the enumeration of attached bacteria and assessment of biofilm disinfection. J. Microbiol. Methods **17:**167–180.
34. **Zhang, T. C., and P. L. Bishop.** 1994. Density, porosity, and pore structure of biofilms. Water Res. **28:**2267–2277.

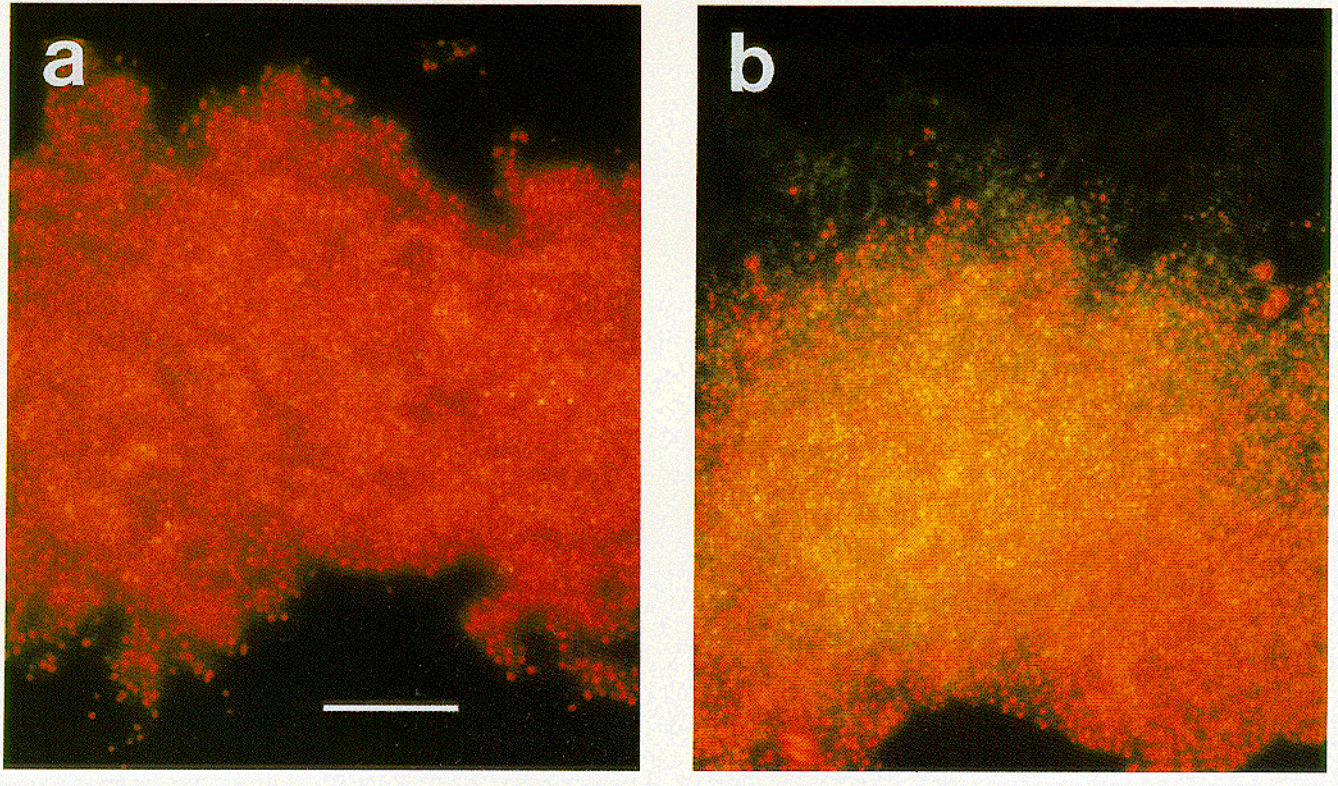
a
b

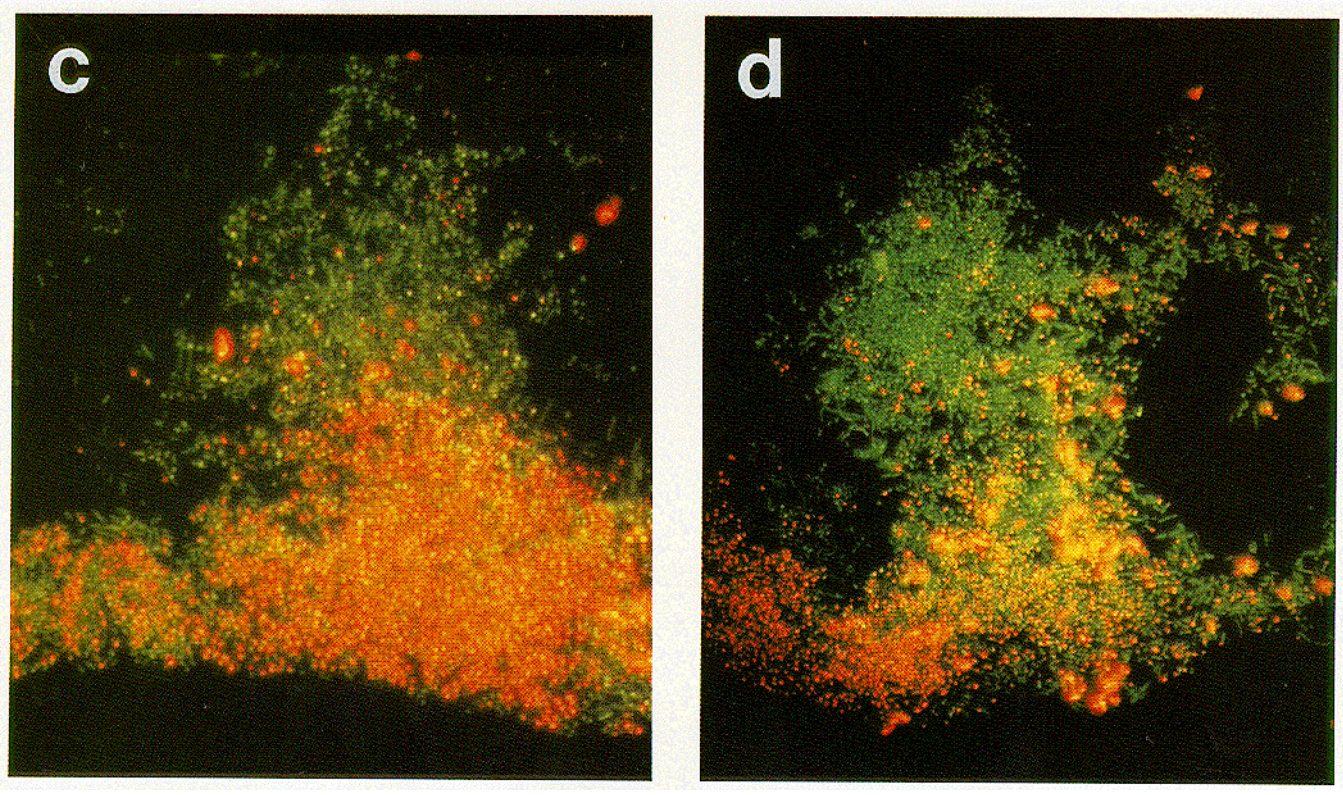
c
d